Local Electrostatics within a Polyelectrolyte Multilayer with Embedded Weak Polyelectrolyte

Anne Feng Xie and Steve Granick*

Department of Materials Science and Engineering, University of Illinois, Urbana, Illinois 61801

Received July 23, 2001; Revised Manuscript Received November 29, 2001

ABSTRACT: We investigate local electrostatics within a polyelectrolyte multilayer formed from layer-by-layer self-assembly of QPVP/PSS (quaternized poly(vinylpyridine)/poly(styrenesulfonate)), through the strategy of embedding, within this multilayer, a weak polyacid, PMA (poly(methacrylic acid)). The methods mainly involved infrared measurements of these multilayer films using FTIR-ATR, Fourier transform infrared spectroscopy in attenuated total reflection, after deposition at several solution concentrations and ionic strength. A key finding is that the ionization of PMA, measured at pH = 6.0 (near its pK_a), executed giant oscillations, between 30% and 80% ionization, each oscillation being in linear proportion to the quantity of strong polyelectrolyte deposited in the outermost layer of the polyelectrolyte multilayer. These oscillations persisted with a decay length (>10 layers) that far exceeded the Debye length of the aqueous solution, suggesting that this long-range electrostatic coupling stemmed from the presence of polyanions and polycations that were fixed in space within the multilayer assembly rather than mobile as supposed in a traditional analysis of screening. In addition, in the process of multilayer formation, the mass adsorbed of the outermost layer was not simply controlled by the excess charge on the preexisting multilayer. Instead, the film became responsive in the sense that its charge adjusted in the direction of maintaining neutrality within the multilayer assembly when additional charges deposited on top. The approach of embedding a weak polyelectrolyte within a multilayer of strong polyelectrolyte may find application in sensor design.

Introduction

For decades, organic thin films have comprised potential materials applied to various interdisciplinary areas. To control molecular organization and orientation on a nanoscopic level, a new method was introduced by Decher et al. for the formation of multicomposite films through layer-by-layer-deposition of oppositely charged polyelectrolytes.[1] The versatility of this technique provides the opportunity to manipulate nanoscopic structure of a macroscopic device. Since then, applications of the electrostatic-assembly technique have blossomed, for example, in the fields of biosensors, light-emitting diodes, nonlinear optical devices, and permselective gas membranes.[1−8]

Most of the work to date concerns the use of "strong" polyelectrolytes, whose charge is fixed.[9−12] Fewer studies concern "weak" polyelectrolytes, whose charge responds to the local electrostatic environment by the chemical equilibrium known as ionization. In this respect, the use of weak polyelectrolytes widens the window for manipulation of molecular organization.[4,13−20]

Open questions addressed in the following study include the following. What controls the mass of polyelectrolyte adsorbed in each layer? How does the local environment (pH and dielectric constant) influence electrostatic interactions? How does the ionization equilibrium respond to these variables? Note that measurements of the local electric field and local environments are rare, apart from a recent experiment in which the proton concentration profile within a polyelectrolyte film was inferred using a pH-sensitive fluorescent label.[21]

In this paper, we investigate these issues through the strategy of embedding, within the multilayer, a weak polyacid whose charge density responds to changes of the local environment. In previous work, we established the feasibility of using Fourier transform infrared spectroscopy (FTIR) in the mode of attenuated total reflection (ATR) to study adsorption of weak polyelectrolytes at the surface of an infrared prism.[22] The infrared technique was found sensitive to monitor not only the total mass adsorbed but also the mass of discrete chemical species within a mixture as well as their ionization. A preliminary communication of this work was presented previously.[19]

Experimental Section

Experiments were performed at 25 °C, and the pH was usually fixed at 6.0. The concentration of the polyelectrolyte solutions used for multilayer formation was either 1 mg mL^{-1} (with salt concentration of 0.1 or 1 M) or 0.01 mg mL^{-1} (with salt concentration of 5 mM). Figure 1 shows the composition of the multilayer that we studied. Five bilayers of QPVP/PSS were built on top of a precursor bilayer of QPVP/PMA. These acronyms are defined in the Materials section.

Materials. The cationic polymer was fully quaternized poly(vinylpyridine) (QPVP). The parent PVP samples (M_w = 34 000, M_w/M_n = 1.23) were purchased from Polymer Source, Quebec, Canada. The procedure to quaternize PVP with an excess of ethyl bromide was described elsewhere.[23] The proportion of alkylated units in the yielded polymer was 100%, as determined by infrared spectroscopy. The anionic polymers used were poly(styrenesulfonate) (PSS, M_w = 35 000, M_w/M_n = 1.1) purchased from Polymer Laboratories, Church Stretton, UK, and poly(methacrylic acid) (PMA, M_w = 40 000, M_w/M_n = 1.02) obtained from Polymer Standards Service, Mainz, Germany. Both were in the form of sodium salt and used without further purification. Spermine was purchased from Sigma (St. Louis, MO) and used as received.

To control pH and ionic strength, the inorganic salts Na_2HPO_4 and $NaH_2PO_4{\cdot}H_2O$ (General Storage, pure grade) were used as received. The H_2O used for glassware cleaning was double distilled and further purified by passage through a deionizing Milli-Q system (Millipore).

Experiments were carried out in D_2O rather than H_2O to reduce overlap of the infrared (IR) spectra of carboxylate band

10.1021/ma011293z CCC: $22.00
Published on Web 01/18/2002

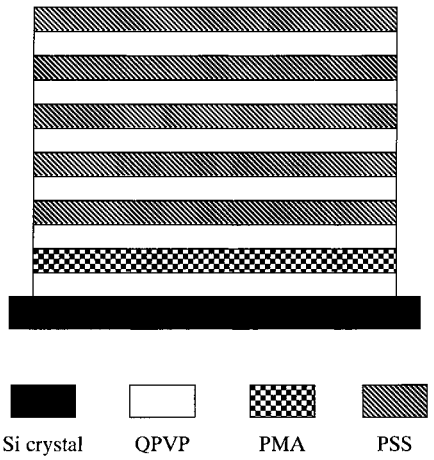

Figure 1. Structure of the multilayers that were investigated. First, a layer of polycation (QPVP) was deposited from dilute solution onto the initially bare surface of a Si ATR crystal carrying negative charge from dissociated silanol groups. The second layer was comprised of a weak polyacid, PMA. After the adsorption of PMA had equilibrated, alternate layers of QPVP and of polyanion, PSS, were deposited sequentially from dilute solution. The cartoon shows the multilayers as distinct slabs in order to convey the order of the deposition; it is worth emphasizing that it is known from prior work that interpenetration occurs in practice.

with the strong water band. The D_2O (99.9% isotope content) was purchased from Cambridge Isotope Laboratories and used as received.

Surface Preparation and Polyelectrolyte Multilayer Formation. Multilayer films, mounted within the adsorption cell described elsewhere,[24] were deposited onto a polished Si (111) ATR (attenuated total reflection) crystal (Harrick Sci. Corp.). This was a rectangular trapezoidal crystal of dimension 50 mm × 20 mm × 2 mm with angle 45° to the incident beam and with 45° angle to the exit infrared beam. Before each experiment, residual polymer from the previous experiment was cleaned from the crystal first by UV−ozone exposure for 1 h. The crystal was then dipped momentarily in 5% HF solution, rinsed copiously with water, and finally treated in a UV−ozone plasma cleaner (Harrick Sci. Corp.) for 5 min to regrow an oxide layer. This protocol results in a reproducible oxide layer for subsequent adsorption studies, as has been characterized elsewhere.[25]

To initiate the experiments, after the oxidized Si crystal was mounted into the adsorption cell, phosphate buffer solution was introduced into the cell. After 2 h of stabilization, background spectra were collected, and then phosphate buffer solution was replaced by polyelectrolyte solutions. By exposure of polyelectrolyte solutions to the Si infrared element inside the adsorption cell, multilayer assemblies of oppositely charged polyelectrolytes resulted from consecutive adsorption steps. Before each addition of oppositely charged polyelectrolyte, the cell was rinsed with pure buffer solution copiously until the polyelectrolyte solution used in the previous adsorption step had been completely displaced.

FTIR-ATR Spectroscopy. Infrared spectra were collected using a Bio-Rad FTS-60A Fourier transform infrared spectrometer (FTIR) equipped with a mercury−cadmium−telluride (MCT) detector. Measurements were performed using nonpolarized light, and interferograms were collected with 4 cm^{-1} resolution. Each absorbance spectrum was ratioed to a corresponding background: (1) backgrounds measured with D_2O buffer solution containing the same concentration of inorganic salts as in the sample solution and (2) backgrounds taken with the Si crystal covered with the polymer film formed in the previous deposition steps. Therefore, two kinds of spectra were acquired: (1) spectra of the entire polymer film deposited on the Si crystal and (2) spectra of the top polymer layer. These different methods of analysis were consistent as shown by the fact that the amount adsorbed and ionization that deduced from these two approaches agreed within 5%.

Calibration of the amounts adsorbed was based on measuring the infrared absorbance of known quantities of vibration modes in solution and followed the approach described previously.[26] It was based on integrating the product of the amplitude of the evanescent wave and the concentration of the adsorbing species as a function of distance from the crystal surface, yielding the integrated absorbance of the relevant IR peak.[27,28] Given the 45° angle of incidence for the Si crystal that we used, the penetration depth of the evanescent wave was 0.46, 0.47, and 0.51 μm at 1701, 1643, and 1554 cm^{-1} wavenumbers, respectively. Calibration of the amount of adsorbed QPVP was described in detail elsewhere.[23]

To determine the calibration for PMA, measurements were performed at various pH but the same PMA concentration in order to directly evaluate the extinction coefficients of the carboxylate band, $\nu(COO^-)$, and the carboxylic band, $\nu(C{=}O)$. Results showed no difference between them. For the 50 mm × 20 mm × 2 mm Si crystal used in these experiments, the following calibration constants were obtained: 2870 and 13 824 abs unit m^2 mol^{-1} for QPVP and PMA, respectively.

One might notice that the penetration depth of evanescent wave (around 0.5 μm for the Si crystal that we used) was large compared with the thickness of the adsorbed polymer layers. Hence, the signal we collected included contributions from both free polymers in the solution and adsorbed polymer. To separate these contributions, additional spectra were taken when we replaced the polymer solution with pure buffer solution after each deposition step. In this case, only the molecules irreversibly bound to the surface contributed to the infrared signal. The comparison of those two spectra showed that the contribution of the polymer in the bulk was less than 10% of the total signal for a polymer solution with concentration of 1 mg mL^{-1} and was negligible for a solution concentration of 0.01 mg mL^{-1}. Direct subtraction of the calibrated contribution of polymers in free solution is also possible.[29]

Ellipsometric Measurements. Measurements concerning dry films of polyelectrolyte multilayers were carried out using a Gaertner model L116C ellipsometer with He/Ne laser at 70° angle of incidence. All samples were dried with N_2 for at least 5 min and stored in ambient air before measurement. The thickness of multilayer films was calculated using Gaetner software assuming a refractive index of 1.50 for polymer layers.

Results and Discussion

Representative Spectra. As mentioned in the Experimental Section, to reduce overlap of the infrared spectra of QPVP, PMA, and PSS with those of water itself, we used D_2O rather than H_2O as the solvent. Control experiments showed that our results presented below did not depend on the choice of solvent, H_2O or D_2O.[30]

Figure 2 shows the infrared spectra of PMA molecules in aqueous solutions at pH = 2.0 and 6.0, respectively. Solutions of PMA were exposed to the surface of a Si ATR crystal. Control experiments showed that no PMA adsorbed onto the bare Si crystal surface. Therefore, the plotted absorbance against wavenumber resulted from the free PMA molecules in solution.

The broad peak at 1701 cm^{-1} was assigned to the symmetric stretching vibrations of the carbonyl group, $\nu(C{=}O)$, while the peak at 1554 cm^{-1} was identified as the asymmetric stretching vibrations of the carboxylate anion, $\nu_{as}(COO^-)$. As noted in the Experimental Section, we have verified that the calibration constants for these two vibrations are identical. With the change of pH, the relative intensity of these two peaks varied while the total intensity remained constant. Hence, charge density of this weak polyelectrolyte PMA could be determined quantitatively from the absorbance ratio of these two peaks.

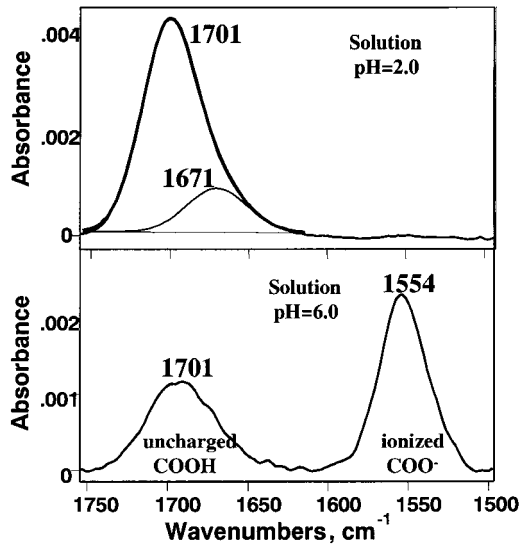

Figure 2. Representative FTIR-ATR spectra of poly(methacrylic acid) (PMA) acquired in situ in aqueous environment. Absorbance is plotted against wavenumber. The PMA in this experiment was at concentration 10 mg mL^{-1} in buffered D_2O solution at pH = 2.0 (top panel) and pH = 6.0 (bottom panel). The absorption bands at 1701 and 1554 cm^{-1} correspond to not ionized and ionized forms of carboxylic groups. They were used to determine fractional ionization and amount of PMA deposited within a multilayer. The composition of the buffer solution was 0.01 M HCl (top panel) or 0.01 M phosphate buffer (bottom panel).

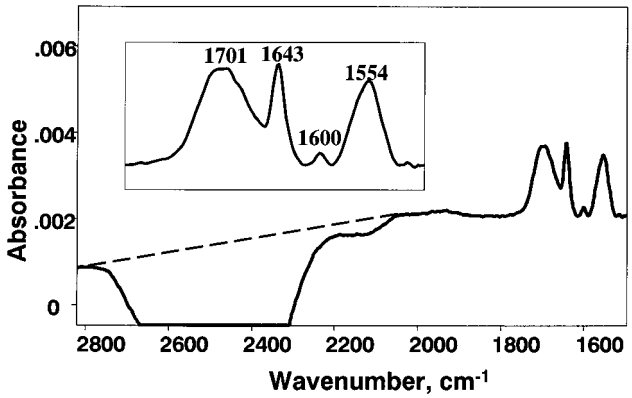

Figure 3. Representative FTIR-ATR spectra acquired in situ in aqueous environment for two bilayers of (QPVP/PSS) with an underlying bilayer of (QPVP/PMA). Absorbance is plotted against wavenumber. The measurement was obtained by ratioing the spectrum of the adsorbed layers in the presence of buffer solution to that of D_2O in pure buffer solution. The intense negative D_2O band (centered at 2480−2500 cm^{-1}) reflects displacement of D_2O from the near-surface region by positive adsorption of polyelectrolyte species, which is magnified in the inset. In the D_2O region of the spectrum, the dotted line shows the baseline.

It has been reported that the vibrations of a monomeric uncharged carboxylic group usually appear at frequencies much higher than 1700 cm^{-1}.[31] There are two possible reasons for our observation of carboxylic group at low frequency. For melts of poly(carboxylic acid)s, peaks centered at around 1700 cm^{-1} have been observed due to the associated or dimerized form of carboxylic groups.[32,33] It is conceivable that some carboxylic groups still remain in associated form when PMA molecules are dissolved in water. At the same time, the solvent effect on vibrational shifts cannot be excluded.[34] It is also possible that the hydrogen bonding of carboxylic groups with D_2O molecules may cause shift of the C═O vibrations to somewhat lower frequencies.

It is also interesting to notice that the shape of the 1701 cm^{-1} peak is slightly asymmetric, broadened to the lower frequencies. The origin of this low-wavenumber peak broadening was discussed in detail elsewhere.[35] For simplicity in curve fitting, we introduced a notional vibrational band at 1671 cm^{-1} to represent those low-energy bands.

Figure 3 gives the in situ infrared spectrum of four layers of polyelectrolyte film composed of QPVP, PMA, QPVP, and PSS, sequentially, ratioed to the background of pure buffer solution without polymers. Absorbance in the infrared region is plotted against wavenumber. The intense negative absorbance from D_2O in the region of 2300−2700 cm^{-1} reflects that D_2O was displaced by the adsorption of polyelectrolytes from the near-surface region. Its strong intensity comes from strong infrared absorptivity of D_2O. This broad band became progressively more negative with the growth of multilayer. It has been reported, from a study of multilayers of poly(ethylenimine) and poly(acrylic acid), that the intensity of the water band was modulated in dependence of the adsorption step due to the alternating hydratability of the outermost layer.[15] In the present system, this was not observed. The linear absorbance decrease of the negative D_2O band not only implies stepwise growth of the polyelectrolyte multilayer but also suggests that the water content within the multilayer film was constant regardless of the addition of more layers.

In Figure 3, the inset magnifies vibrations representing QPVP, PMA, and PSS. The peak centered at 1643 cm^{-1} stands for the charged (quaternized) pyridine ring. Since PVP was quaternized to completion, no peak centered at 1604 cm^{-1} for the neutral ring was observed. The peak centered at 1600 cm^{-1} came from the vibrations of aromatic ring residing in the pendant groups of PSS.[31] The vibrations of sulfonate anion groups are reported to appear at 1200 cm^{-1} (asymmetric) and 1040 cm^{-1} (symmetric),[36] which are out of the frequency range measurable with a Si ATR crystal (opaque at wavenumbers below 1500 cm^{-1}). The intensity of the vibrations at 1600 cm^{-1} was small but could be integrated quantitatively.

The intensities of these different peaks were integrated by curve fitting using Gram32 software in the manner described in detail elsewhere.[23] Briefly, for curve fitting a parameter file was used to fix band centers and widths as well as the Gaussian-to-Lorentzian ratio for each band. The same parameters were applied to all the spectra for consistency. In addition, for calculation of surface excess and ionization of PMA, the spectrum of pure QPVP was subtracted from the multilayer spectra to eliminate its partial overlap with uncharged carboxylic vibrations. Similar operations were applied to calculate surface excess of QPVP molecules.

Adsorption Kinetics. FTIR-ATR experiments were conducted in situ to follow the self-assembly process of the multilayers. Figure 4 shows the time evolution of QPVP amount adsorbed within the first four layers. The deposition was carried out using 0.01 mg mL^{-1} QPVP solution at pH = 6.0. In this process of multilayer buildup, two different kinds of adsorption for QPVP occurred. One was the initial adsorption of the first layer of QPVP onto flat, nonporous, negatively charged bare Si oxide. The other was the deposition of QPVP onto the rough surface comprised of a previously adsorbed

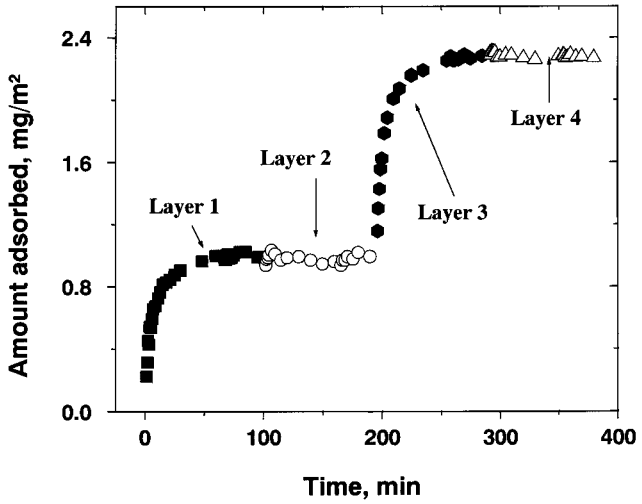

Figure 4. Mass of QPVP adsorbed during the first four deposition steps, plotted against time. During the first and third steps (filled symbols), QPVP molecules accumulated at the surface, while adsorption of polyanions occurred in the second and fourth steps (open symbols). QPVP, PMA, and PSS solutions with concentration 0.01 mg mL^{-1} and phosphate salt concentration of 5 mM were used.

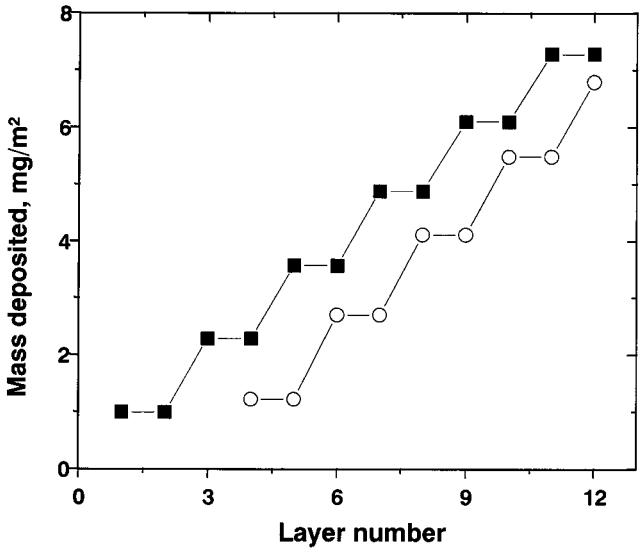

Figure 5. Illustration of layer-by-layer deposition, on top of an embedded layer of weak polyacid, PMA, of alternate layers of polycation and polyanion, QPVP and PSS. The mass deposited, measured in situ by FTIR-ATR, is plotted against layer number for QPVP (filled symbols) and PSS (open symbols). The calculation of the deposited amounts is described in the Experimental Section. First, to prime the surface for subsequent layer-by-layer deposition, QPVP was allowed to adsorb from 0.01 mg mL^{-1} to the surface of the oxidized Si crystal in 5 mM buffer at pH = 6.0. PMA was allowed to adsorb on top and then alternate layers of QPVP and PSS, always from 0.01 mg mL^{-1} solution. Solutions were rinsed with pure buffer between these adsorption steps.

layer of negatively charged polymer chains. For both cases, 80% of the surface coverage was completed during the first 10 min. After 1 h, the adsorption process reached a near-steady state, and no significant increase of amount in QPVP adsorbed layer was observed afterward. Our study shows that similar kinetics of QPVP adsorption occurred for all deposition steps in the course of multilayer growth, indicating that the deposition process had no or little dependence on substrate.

From the curve, the mass in QPVP adsorbed layer remained constant as negatively charged polymer layer was deposited on the top. This demonstrates that no desorption occurred when the adsorbed layer of QPVP was exposed to solution containing negatively charged polymers. Also, no desorption was found at higher polymer concentration (1 mg mL^{-1}, a concentration more than sufficient to complete full surface coverage) at ionic strength of 0.1 M (data not shown here). However, the adsorption of polymer from higher concentration (1 mg mL^{-1}) was much more rapid, surface coverage reaching a pseudo-plateau in less than 1 min, too fast for us to detect the initial stage of adsorption. Experiments showed that the adsorption kinetics of PMA and PSS was similar. For experiments performed from 0.01 mg mL^{-1} polymer solutions, the adsorption was terminated after an hour. The polymer solutions were then exchanged for phosphate buffer solutions with pH controlled at 6.0. For experiments using 1 mg mL^{-1} polymer solutions, the process was interrupted within 30 min.

Stepwise Growth of the Multilayer. The procedure to build up multilayers was the following. First, a layer of QPVP was deposited from dilute solution onto the initially bare surface of a Si ATR crystal carrying negative charge from dissociated silanol groups. This caused surface charge to switch from negative to positive.[23] The second layer was comprised of a weak polyacid, PMA. After the adsorption of PMA equilibrated, alternate layers of QPVP and PSS were deposited sequentially from dilute solution. To eliminate the possibility of charge−charge complex formation in solution, solutions containing polyelectrolytes were rinsed away with pure buffer solutions between successive adsorption steps. Spectra collected before and after rinsing showed no decrease of peak intensity. Figure 5 shows the fidelity of layer-by-layer deposition. These in situ experiments show that the multilayer grew in a stepwise fashion.

Figure 6 describes the consecutive adsorption of QPVP (top panel) and PSS (bottom panel). For both polyelectrolytes, the mass adsorbed grew linearly with the layer number, which demonstrates that the process of multilayer deposition was the same from layer to layer. The three curves represent adsorption from polyelectrolyte solutions whose concentration and ionic strength were different; the different slopes show a strong dependence on polymer concentration and ionic strength. From solution concentration of 0.01 mg mL^{-1}, the amount deposited was 1.3 mg m^{-2}. When the solution concentration was increased 100-fold to 1 mg mL^{-1}, the amount increased to 2.0 mg m^{-2} per layer.

Since the salt concentration in these two cases was different, 5 mM for the most dilute solution and 0.1 M for the other one, we cannot exclude an influence of ionic strength. In fact, we expect this, especially for high polymer concentrations. Figure 6 shows the influence of ionic strength on the amount adsorbed per layer at concentrations above the plateau of the adsorption isotherm: the average amount per layer doubled when salt concentration was increased from 0.1 to 1 M.

This observation is consistent with earlier work[37] that ionic strength plays in the process of multilayer growth, especially in the case of high salt concentration. Apparently this is a substrate effect. For the first layer, its substrate is bare solid surface, smoother than the surface covered by polymer chains. In past work by others, lesser amounts adsorbed have been observed for

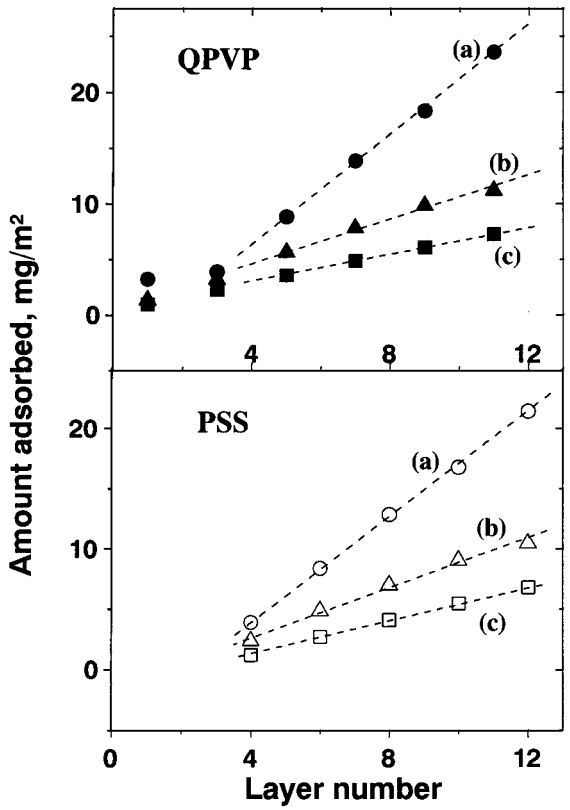

Figure 6. Successive adsorption of QPVP (top panel) and PSS (bottom panel) from pH = 6.0 phosphate buffer solution onto oxidized Si. The mass adsorbed of QPVP (top panel) and PSS (bottom panel) is plotted against layer number. Odd layer numbers are the QPVP adsorption step; even layer numbers are the PSS adsorption step. (a) Adsorption from 1 mg mL^{-1} QPVP solution (solid symbols) and PSS solution (open symbols) with phosphate salt concentration of 1 M. (b) Adsorption from 1 mg/mL QPVP solution (solid) and PSS solution (open) with salt concentration of 0.1 M. (c) Adsorption from 0.01 mg mL^{-1} QPVP solution (solid) and PSS (open) with salt concentration of 5 mM.

the first layer.[39] In our system, no distinct difference of adsorbed amount was found for multilayer formed from solutions with low salt concentration, which means surface roughness had little effect. On the contrary, an enhancement of amount adsorbed in the first layer was observed for the cases of high salt concentrations, and the effect was magnified by the increase of ionic strength. This can be explained by electrostatic screening effect of salts. When ionic strength in solution was high, both electrostatic repulsion between segments of the adsorbed chains and attraction between segments and surface were weakened, and chains became flexible enough to adopt fluffier conformation with more loops and fewer trains. Therefore, the efficiency of surface charge compensation was suppressed by binding of small ions together with loops. On the other hand, when polyion chains were exposed to a "softer" surface covered by preadsorbed polymers, surface charge compensation could be accomplished effectively by interpenetration of polymeric chains. As a result, the amount adsorbed for the first layer was enhanced.

Previous polyelectrolyte adsorption studies found that thinner layers resulted, owing to kinetic limitation,[40] from lowering the solution concentration of the polyelectrolyte. To test this idea in the present systems, ellipsometric measurements were carried out to observe thickness of dried films as a function of adsorbed

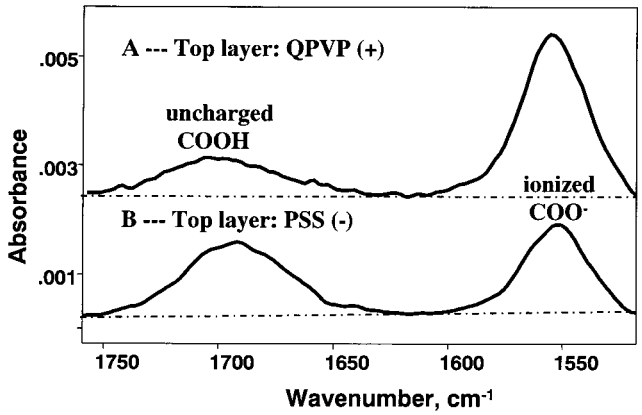

Figure 7. Infrared spectra for embedded PMA layer with consecutive adsorption of QPVP and PSS: spectrum A, third deposition step when adsorption of QPVP occurred; spectrum B, fourth deposition step when a layer of PSS molecules was introduced onto the surface. The relative intensity changes of the charged carboxylate groups (centered at 1554 cm^{-1}) and uncharged groups (centered at 1701 cm^{-1}) of PMA reflect the ionization changes in response to charge variations of the top layer.

Table 1. Thickness and Mass Adsorbed per Bilayer of QPVP/PSS Multilayers Formed from Polyelectrolyte Solutions with Different Concentration and Ionic Strength

polymer concn (mg mL^{-1})	NaCl concn (M)	dry thickness (nm per bilayer)	adsorbed amount (mg m^{-2})
0.01	0.005	1.6	2.6
1	0.1	3.0	4.0
1	1	6.4	7.2

amount. After every IR experiment, the Si crystal covered by polyelectrolyte multilayer was taken out from the cell, rinsed with water, and blowed with dry N_2 for at least 5 min. Then the total thickness of multilayer film was measured by ellipsometry. The thickness per polycation/polyanion bilayer was obtained by dividing the total thickness of the film by its bilayer number.

Table 1 compares the average thickness and adsorbed amount per bilayer for three different fabrication processes of multilayer films. Assuming that the density of dry organic film was approximately 1 g cm^{-3}, our thickness measurements of multilayer films made from high-concentration polymer solutions (the second and third cases in Table 1) agree well with the adsorbed amounts obtained by IR experiments. There is some discrepancy in case 1, indicating some conformation difference from cases 2 and 3. Presumably, solutions with low concentration of polymers gave rise to films with higher density. Another contribution may come from low ionic strength. Under these circumstances, polymers adopted flatter conformations when they adsorbed.

Ionization Changes of Embedded PMA. 1. Ionization Oscillation. The ionization of adsorbed PMA can be modulated by changing the surface electrical potential;[41] as described above, a layer of PMA molecules was embedded at the bottom of multilayer in order to investigate local electrostatics. Figure 7 compares the intensity ratio of the charged and uncharged carboxylic groups upon the addition of strong (fully charged) polyelectrolytes. The ionization of PMA in the embedded layer oscillated with the net charge of the outermost layer.

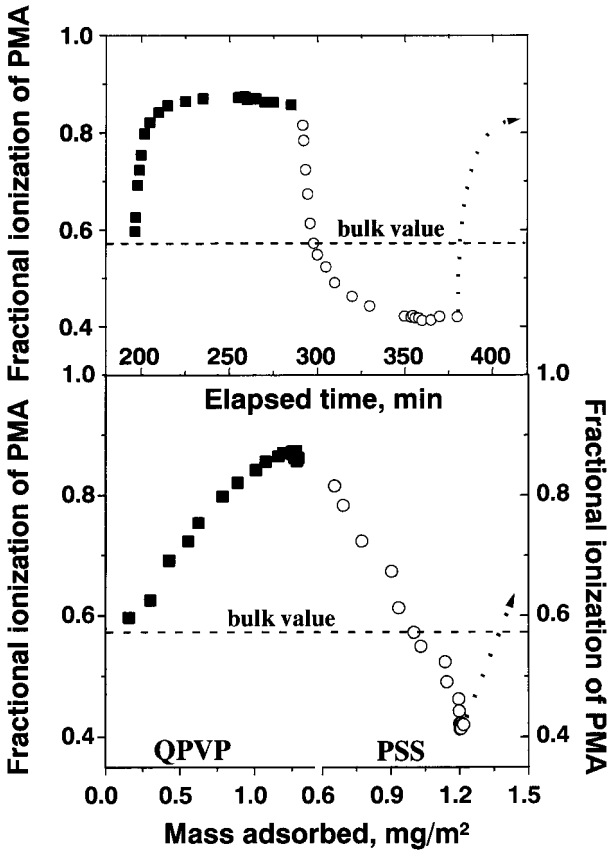

Figure 8. Fractional ionization of PMA plotted against time elapsed during subsequent deposition of a QPVP and then a PSS layer on top (top panel) and, equivalently, against mass adsorbed during this process (bottom panel). Dashed lines show ionization in bulk solution. Polymer solutions of concentration 0.01 mg mL^{-1} with phosphate salt concentration of 5 mM buffered at pH = 6.0 were used.

According to classical expectation,[42] this should stem from the local electrostatic potential. The local electric field results in a local distribution of ions (protons), which in turn changes the local pH, leading to a local ionization in response to the local pH. Therefore, if surface potential is negative (curve B), protons are enhanced near the surface, which means the pH at the surface is lower than that in the bulk; on the other hand, the pH at the surface is higher if the surface potential is positive (curve A). The local pH can be estimated by the relation[42]

$$pH_s = pH_\infty + \frac{e\Psi_s}{2.3kT} \quad (1)$$

where pH_s is the pH value at the surface, pH_∞ is the value in the solution, and Ψ_s is the surface potential.

The remarkable finding is that ionization of the embedded polyacid oscillated with net charge of the electrostatic multilayer on top. The top panel of Figure 8 illustrates the ionization of PMA plotted against elapsed time, first during the deposition of the strong polycation (QPVP) on top and next during the deposition of the strong polyanion (PSS) on top of this. The positively charged overlayer first induced enhanced negative charge on PMA, but the subsequent overlayer of opposite charge suppressed this ionization to a level below the value in bulk solution. The bottom panel of Figure 8 shows that ionization changed in almost linear proportion to the quantity of polycation and polyanion deposited, implying the linear relation between ionization change and surface potential.

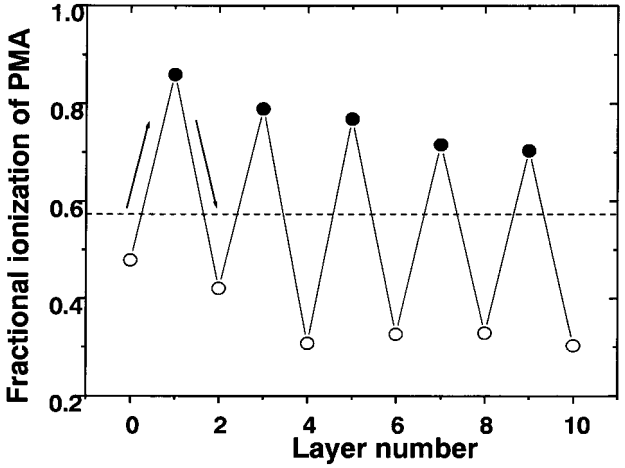

Figure 9. Fractional ionization of embedded PMA plotted against number of layers of strong polyelectrolyte (PSS and QPVP) deposited on top. The minima of the oscillations show no systematic dependence on layer number. The maxima decay with an extraordinarily slow decay length of ≈10 layers. Polymer solutions with concentration 0.01 mg mL^{-1} and phosphate salt concentration of 5 mM buffered at pH = 6.0 were used. The horizontal dashed line shows the ionization of PMA in the bulk solution at this pH.

We studied ionization changes of the PMA embedded layer as multiple additional layers of strong polyelectrolyte were allowed to adsorb on top. The ionization of the PMA embedded layer oscillated with layer number, as shown in Figure 9. The remarkable point is that fractional ionization appeared to be affected by the outer charges although the immediate environment (strong polyelectrolyte layers sandwiched between top layer and embedded polyacid layer) did not change. Ionization oscillation persisted up to the thickest films investigated (a further 10 layers of electrostatic multilayers on top of the embedded layer). The magnitude of the oscillation was large—the ionization level changed by a factor more than 2, between ≈30% and 80%, as successive layers were added. Their maxima decayed slightly with increasing layer number. The minima of oscillation showed no systematic dependence on layer number.

2. Salt Concentration Effect. To further explore the effect of surface electric field, multilayers made from solutions with higher salt concentration were also studied. A comparison of two different multilayer films—formed from solutions with salt concentrations of 5 mM and 0.1 M—is given in Figure 10. Ionization of PMA is plotted against the distance between PMA embedded layer and the outermost layer (estimated from ellipsometric measurements). The remarkable point is that even for films in the environment of high ionic strength, the oscillations of ionization extended to more than 10 layers. Apparently, the electrostatic interaction could not be screened by small ions even when bulk salt concentration was as high as 0.1 M (Debye length of 1 nm).

On the basis of the Gouy−Chapman-Stern model,[40] the local pH value is described by eq 1. From this equation and the calibrated relation between solution pH and ionization of PMA in solution,[41] one can estimate the average values of surface pH and in turn electric potentials that PMA experienced after consecutive deposition steps. The dashed line in the top panel of Figure 10 implies that within the multilayers the

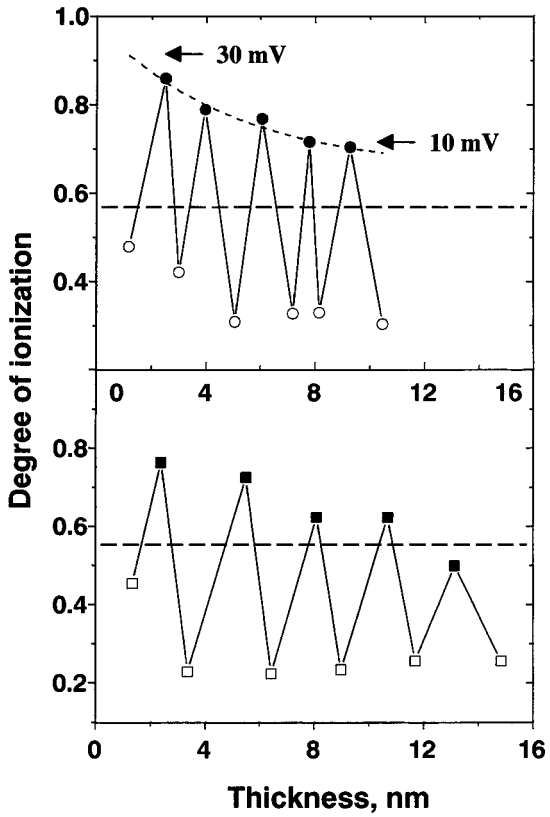

Figure 10. Fractional ionization of embedded PMA layer plotted as a function of film thickness: top panel, adsorption from 0.01 mg/mL QPVP, PMA, and PSS solutions with phosphate salt concentration of 5 mM; bottom panel, adsorption from 1 mg mL^{-1} QPVP, PMA, and PSS solutions with phosphate salt concentration of 0.1 M. Horizontal dashed lines show ionization in bulk solution. Curved dotted line illustrates how the electric potential experienced by the embedded PMA layer, estimated from eq 1, decays as a function of distance within multilayer.

potential distribution decayed exponentially as a function of distance but with decay length much larger than that predicted by classical DLVO theory. From the plot, we can estimate the decay length (where potential decreases to e^{-1} of the original value) to be more than 6 nm, whereas any traditional estimate (Debye length) is much smaller. In addition, bearing in mind that the thickness was determined from ellipsometric measurements on dry layers and that the wet layers were doubtless swollen by water, the actual decay length was even larger.

Our speculation is that the ionic strength (owing to mobile ions) inside the multilayers was much less than in the bulk. Small ions were either excluded from the multilayer or localized along the polymeric chains, so that the screening of electrostatic interaction by small mobile ions became a minor effect. Therefore, it is understandable why the range of oscillation of ionization change of the PMA embedded layer was essentially the same regardless of the ionic strength of the surrounding solution.

Recently, Finkenstadt and Johnson presented a theoretical model to explain this observation by treating the multilayer film as an ionic solid of alternating positive and negative charge.[43] Their model suggests that the larger decay length observed in these experiments originate because electrostatic complexes between polycations and polyanions are fixed in space—not mobile as is normally supposed in a colloid analysis of electrostatic screening.[44] From the calculation of decay length of surface potential of multilayer, the low local ionic strength of 10^{-3} M was estimated. This is consistent with the finding by several groups that free inorganic ions have very low abundance within electrostatic multilayers,[45,46] indicating near stoichiometry between the polyanions and polycations.

Another possible contribution stems from hydrophobicity of chemical moieties within the multilayer, which may lower the local dielectric constant below that of bulk water. In fact, when we are dealing with molecularly thin films, the continuum notion of dielectric constant to represent electric polarization property of the bulk material may be expected to be no longer a constant and perhaps no longer isotropic. Therefore, we refer to the effective dielectric constant, ϵ_{eff}, characteristic of the dielectric screening of electrostatic interaction in the local environment. Studies have shown a difference in dielectric screening in aqueous solutions for organic acid[47] and proteins.[48] It was inferred that the screening of backbone−dipole interactions inside the helix of protein was much less effective than for charges in free aqueous solution, with an effective dielectric constant as low as 8.[48] It is reasonable to expect an analogous decrease in the effective dielectric constant for multilayers. This in turn raises many questions, especially concerning whether the electric fields coming from inside the multilayer interfere with those from the outermost layer so that the electric field effect of the top layer is weakened. Local probes that respond directly to local electric field are desirable in order to address these issues directly.

Charge Balance. Generally, positive and negative charges cancel. This so-called "charge compensation" for the formation of interpolyelectrolyte complexes in bulk solution is expected and has been demonstrated,[49] but the issue of charge balance within surface-attached multilayers is not yet fully understood.[13,50,51] The investigation carried out by Caruso et al. revealed that charge balance within the multilayer involves both polyions and small ions.[13] The fact that up to 30% of the charge sites on polyions could be bound by oppositely charged fluorescent probes indicated that charge compensation within the multilayer was fulfilled by more than ion-pair binding to oppositely charged sites on the polyions. However, the result was rather qualitative due to the size of the fluorescent probes. The interpenetrating feature of the multilayer might impede the uptake of the large probe molecules—they might find too little space to enter. To understand the extent of charge compensation in our multilayer assembly, we calculated the charge ratio of polyions from the amount adsorbed measured by FTIR-ATR. This study shows that, in the process of multilayer formation, the mass adsorbed of the outermost layer was not simply controlled by the excess charge on the preexisting multilayer. In fact, with a weak polyacid layer woven inside the multilayer, the film became responsive in the sense that its charge adjusted in the direction of maintaining neutrality.

Figure 11 shows the charge ratio of total positive charges to total negative charges of polymer within the multilayer assembly, plotted against layer number. These represent direct IR measurements of the charges on these polymers (but the presence of inorganic ions and protons could not be measured using this technique). The curve with the largest excursions shows the charge ratio for multilayers formed from strong poly-

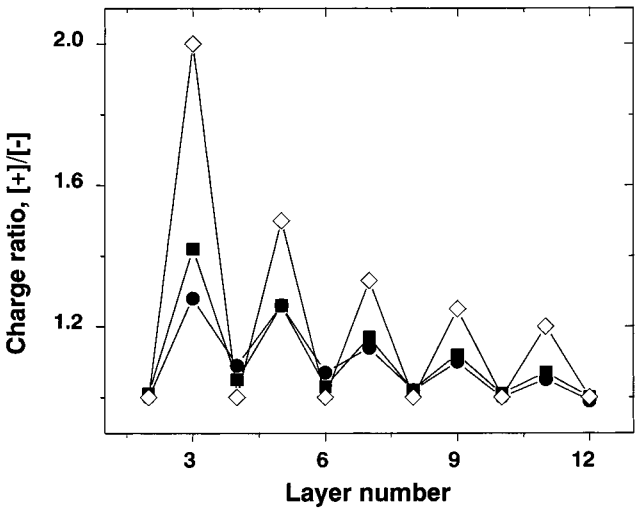

Figure 11. Ratio of positive charges to negative charges of polymer moieties within the multilayer, plotted against layer number. Square symbols represent multilayers made from 1 mg mL^{-1} QPVP, PMA, and PSS solutions with phosphate salt concentration of 0.1 M. Circular symbols represent multilayers made from 0.01 mg mL^{-1} QPVP, PMA, and PSS solutions with phosphate salt concentration of 5 mM. Diamond symbols represent an ideal situation in which the multilayer is composed of only strong polyelectrolytes such that the multilayer achieves 100% charge compensation at each adsorption step. The embedded weak polyacid layer was found to have the chemical capacity to adjust its charge in the direction of maintaining electroneutrality of the multilayer.

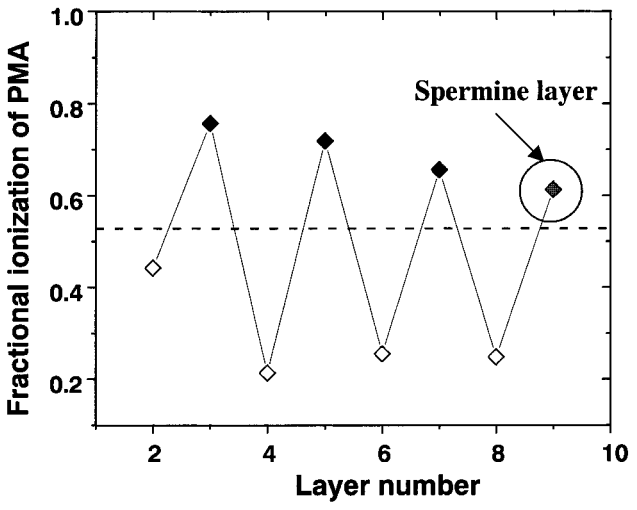

Figure 12. Fractional ionization of embedded PMA plotted against number of layers of either strong polyelectrolyte (open symbol, PSS; solid symbol, QPVP) or spermine (grey diamond) deposited on top. Polymer solutions with concentration 1 mg mL^{-1}, spermine solution with concentration 3 mg mL^{-1}, and phosphate salt concentration of 0.1 M buffered at pH = 6.0 were used. The horizontal dashed line shows the ionization of PMA in the bulk solution at this pH.

electrolytes, assuming that surface charge was fully compensated at each deposition step. The large deviation from unity for the first few polycation layers reflects the fact that the surface charge density of bare Si crystal was not taken into account. As more and more polyions were deposited onto the surface, this mattered less, resulting in total charge balance approaching to unity. Compared with this estimate, a damping of oscillation of charge balance was found for the system with embedded PMA—damping by around 20% (thicker film) to 30% (thinner film). This reflects the additional active influence of the PMA embedded layer; this layer adjusted its ionization in the direction to tending toward electroneutrality. There was long-range coupling between ionization within the embedded weak polyacid and charge deposited on the outermost layer of strong polyelectrolyte, far removed from it in space. Conversely, when charges were added to the outermost layer by depositing other polyions on top, electrostatic changes were induced far away within the interior. By this mechanism, charge balance within the multilayer was regulated in the direction of electroneutrality.

Conclusion and Outlook

This study shows that charge within polyelectrolyte multilayers is not a simple matter of counting the charge introduced by each successive layer. Polyions inside a multilayer that contains weak polyelectrolyte can adjust their charge density, in response to changes of the local electrostatic environment. Therefore, one can predict charge regulation within the multilayer in response to varying pH or electric field. Furthermore, the approach of embedding a weak polyelectrolyte within a multilayer of strong polyelectrolyte may allow us to sense changes in external environmental conditions that act upon the outside of the multilayer assembly. We have verified that ionization behaved in the same manner during the deposition of both spermine (charge +3) (Figure 12) and a charged protein (bovine serum albumin) (result not shown). This may find application in the design of surface sensors for adsorbed ions and polyions.

Acknowledgment. We are indebted to Duane D. Johnson and Dan Finkenstadt (University of Illinois) for suggesting the physical interpretation and to Svetlana A. Sukhishvili (Stevens Institute of Technology) for many discussions. This work was supported by the taxpayers of the United States through the National Science Foundation and by the U.S. Department of Energy, Division of Materials Science, through Grant DEFG02-91ER45439 to the Frederick Seitz Materials Research Laboratory at the University of Illinois at Urbana−Champaign.

References and Notes

(1) Decher, G. *Science* **1997**, *277*, 1232.
(2) Esker, R.; Mengel, C.; Wegner, G. *Science* **1998**, *280*, 892.
(3) Caruso, F.; Caruso, R. A.; Möhwald, H. *Science* **1998**, *282*, 1111.
(4) Shiratori, S. S.; Rubner, M. F. *Macromolecules* **2000**, *33*, 4213.
(5) Clark, S. L.; Hammond, P. T. *Adv. Mater.* **1998**, *10*, 1515.
(6) Husemann, M.; et al. *J. Am. Chem. Soc.* **2000**, *122*, 1844.
(7) Huck, W. T. S.; Strook, A. D.; Whitesides, G. M. *Angew. Chem., Int. Ed.* **2000**, *39*, 1058.
(8) Levasalmi, J.-M.; McCarthy, T. J. *Macromolecules* **1997**, *30*, 1752.
(9) Kellogg, G. J.; Mayes, A. M.; Stockton, W. B.; Ferreira, M.; Rubner, M. F.; Satija, S. K. *Langmuir* **1996**, *12*, 5109.
(10) Hoogeveen, N. G.; Cohen Stuart, M. A.; Fleer, G. J.; Bohmer, M. R. *Langmuir* **1996**, *12*, 3675.
(11) Schlenoff, J. B.; Ly, H.; Li, M. *J. Am. Chem. Soc.* **1998**, *120*, 7626.
(12) Ladam, G.; Schaad, P.; Voegel, J. C.; Schaaf, P.; Decher, G.; Cuisinier, F. *Langmuir* **2000**, *16*, 1249.
(13) Caruso, F.; Lichtenfeld, H.; Donath, E.; Möhwald, H. *Macromolecules* **1999**, *32*, 2317.
(14) Yoo, D.; Shiratori, S. S.; Rubner, M. F. *Macromolecules* **1998**, *31*, 4309.
(15) Muller, M.; Rieser, T.; Lunkwitz, K.; Berwald, S.; Meier-Haack, J.; Jehnichen, D. *Macromol. Rapid Commun.* **1998**, *19*, 333.

(16) Chen, K. M.; Jiang, X. P.; Kimerling, L. C.; Hammond, P. T. *Langmuir* **2000**, *16*, 7825.
(17) Clark, S. L.; Hammond, P. T. *Langmuir* **2000**, *16*, 10206.
(18) Krasemann, L.; Tieke, B. *Langmuir* **2000**, *16*, 287.
(19) Xie, A. F.; Granick, S. *J. Am. Chem. Soc.* **2001**, *123*, 3175.
(20) Dubas, S. T.; Farhat, T. R.; Schlenoff, J. B. *J. Am. Chem. Soc.* **2001**, *123*, 5368.
(21) Klitzing, R. von; Möhwald, H. *Langmuir* **1995**, *11*, 3554.
(22) Sukhishvili, S. A.; Granick, S. *Phys. Rev. Lett.* **1998**, *80*, 3646.
(23) Sukhishvili, S. A.; Granick, S. *J. Chem. Phys.* **1998**, *109*, 6861.
(24) Frantz, P.; Granick, S. *Macromolecules* **1995**, *28*, 6915.
(25) Frantz, P.; Granick, S. *Langmuir* **1992**, *8*, 1176.
(26) Sperline, R. R.; Maralidharan, S.; Feiser, H. *Langmuir* **1987**, *3*, 198.
(27) Harrick, N. J. *J. Opt. Soc. Am.* **1965**, *55*, 851.
(28) Tompkins, H. G. *Appl. Spectrosc.* **1974**, *28*, 335.
(29) Sukhishvili, S. A.; Dhinojwala, A.; Granick, S. *Langmuir* **1999**, *15*, 8474.
(30) Sukhishvili, S. A.; Granick, S. *J. Phys. Chem. B* **1999**, *103*, 472.
(31) Colthup, N. B.; Daly, L. H.; Wiberley, S. E. In *Introduction to Infrared and Ramen Spectroscopy*; Academic Press: New York, 1975.
(32) Lu, X.; Weiss, R. A. *Macromolecules* **1995**, *28*, 3022.
(33) Dong, J.; Ozaki, Y.; Nakashima, K. *Macromolecules* **1997**, *30*, 1111.
(34) Trewhella, J.; Liddle, W. K.; Heidorn, D. B.; Strynadka, N. *Biochemistry* **1998**, *28*, 1294.
(35) Sukhishvili, S. A.; Granick, S. *Macromolecules* **2002**, *35*, 301.
(36) Gregoriou, V. G.; Hapanowicz, R.; Clark, S. L.; Hammond, P. T. *Appl. Spectrosc.* **1994**, *51*, 470.
(37) Lösche, M.; Schmitt, J.; Decher, G.; Bouwman, W. G.; Kjaer, K. *Macromolecules* **1998**, *31*, 8893.
(38) Sukhorukov, G. B.; Schmitt, J.; Decher, G. *Ber. Bunsen-Ges. Phys. Chem.* **1996**, *100*, 948.
(39) Schmitt, J.; Grunewald, T.; Decher, G.; Pershan, P. S.; Kjaer, K.; Losche, M. *Macromolecules* **1993**, *26*, 7058.
(40) Berndt, P.; Kurihara, K.; Kunitake, T. *Langmuir* **1992**, *8*, 2486.
(41) Xie, A. F.; Granick, S., unpublished experiments.
(42) Healy, T. W.; White, L. R. *Adv. Colloid Interface Sci.* **1978**, *9*, 303.
(43) Finkenstadt, D.; Johnson, D. D. *Langmuir*, in press.
(44) Israelachvili, J. N. In *Intermolecular and Surface Forces*, 2nd ed.; Academic Press: London, 1992.
(45) Korneev, D.; Lvov, Y.; Decher, G.; Schmitt, J.; Yaradaikin, S. *Physica B* **1995**, *213 & 214*, 954.
(46) Schlenoff, J. B.; Ly, H.; Li, M. *J. Am. Chem. Soc.* **1998**, *120*, 7626.
(47) Baker, F. W.; Parish, R. C.; Stock, L. M. *J. Am. Chem. Soc.* **1967**, *89*, 5677.
(48) Lockhart, D. J.; Kim, P. S. *Science* **1992**, *257*, 947.
(49) Petrak, K. In *Polyelectrolytes: Science and Technology*; Hara, M., Ed.; Marcel Dekker: New York, 1992.
(50) Wang, X. G.; Balasubramanian, S.; Li, L.; Jiang, X. L.; Sandman, D. J.; Rubner, M. F.; Kumar, J.; Tripathy, S. K. *Macromol. Rapid Commun.* **1997**, *18*, 451.
(51) Laschewsky, A.; Wischerhoff, E.; Kauranen, M.; Persoons, A. *Macromolecules* **1997**, *30*, 8304.

MA011293Z